Journal of Scientific Computing, Vol. 26, No. 2, February 2006 (© 2006)
DOI: 10.1007/s10915-005-4929-2

A Time-Splitting Spectral Method for the Generalized Zakharov System in Multi-Dimensions

Shi Jin[1] **and Chunxiong Zheng**[2]

Received September 21, 2004; accepted (in revised form) January 18, 2005

The generalized Zakharov system (ZS) couples a dispersive field $\mathbf{E}$ (scalar or vectorial) and $\mathcal{J}$ nondispersive fields $\{n_j\}_{j=1}^{\mathcal{J}}$ with a propagating speed of $1/\epsilon_j$. In this paper, we extend our one-dimensional time-splitting spectral method (TSSP) for the generalized ZS into higher dimension. A main new idea is to reformulate the multi-dimensional wave equations for the nondispersive fields into a first-order system using a change of variable defined in the Fourier space. The proposed scheme TSSP is unconditionally stable, second-order in time and spectrally accurate in space. Moreover, in the subsonic regime, it allows numerical capturing of the subsonic limit without resolving the small parameters ϵ_j. Numerical examples confirm these properties of this method.

KEY WORDS: Zakharov system; time-splitting spectral method; subsonic regime; multi-dimensions.

1. INTRODUCTION

This work is aimed at extending the one-dimensional time-splitting spectral method (TSSP), developed in our previous work [17], for a more general form of the Zakharov system (ZS) in higher dimension:

$$i\mathbf{E}_t - \alpha\nabla\times(\nabla\times\mathbf{E}) + \nabla(\nabla\cdot\mathbf{E}) + \lambda|\mathbf{E}|^2\mathbf{E} + \sum_{j=1}^{\mathcal{J}} n_j\mathbf{E} = 0, \tag{1}$$

$$\epsilon_j^2 n_{j,tt} - \Delta n_j + \mu_j\Delta|\mathbf{E}|^2 = 0, \quad \forall j = 1,\ldots,\mathcal{J}. \tag{2}$$

[1] Department of Mathematics, University of Wisconsin, Madison, WI 53706, USA and Department of Mathematical Science, Tsinghua University, Beijing 100084, P.R. China. E-mail: jin@math.wisc.edu
[2] Department of Mathematical Science, Tsinghua University, Beijing 100084, P.R. China. E-mail: czheng@math.tsinghua.edu.cn

In the ZS system, the complex, dispersive field $\mathbf{E}$, either scalar or vectorial, is the varying envelope of a highly oscillatory electric field, and the real, nondispersive field n_j is the fluctuation of the plasma ion density of jth species from its equilibrium state. The parameters $\alpha, \lambda, \epsilon$ and μ_j are all real numbers. The generalized ZS is a rather universal model to govern the interaction between dispersive and nondispersive waves, not only in plasma physics, but in many other research areas also, such as hydrodynamics [10] and molecular chains [9].

During the past two decades, many numerical methods have been proposed to solve this kind of systems. For example, Payne *et al.* [20] designed a spectral method for a one-dimensional ZS. Glassey [12] presented an energy-preserving finite difference scheme for the ZS in one-dimension, and later proved its convergence in [13]. Chang *et al.* [7,8] presented a conservative difference scheme for the generalized ZS and proved the convergence of their method.

Motivated by the TSSP for the linear and nonlinear Schrödinger equation (see, e.g., [18]), which was shown to be particularly effective in the semi-classical regime [1,2], Bao *et al.* [4] proposed a TSSP to solve the generalized one-dimensional ZS. Their method was later extended to the ZS for multi-component plasma [3]. In the subsonic regime, where some $\epsilon_j \ll 1$, these methods require mesh size and time step to be the order of ϵ_j. This constraint was removed, for the first time, in our previous work in [17], where a different TSSP was developed allowing the numerical capturing of the subsonic limit with numerical mesh size and time step *independent of* ϵ_j. A main ingredient of our method was to first formulate the second-order wave equation for the nondispersive field into a first-order system, which is then discretized in time by the Crank–Nicolson method, which, amazingly, outperforms the exact time integration in the subsonic regime.

In this paper, this idea is extended into higher space dimension. While we follow the same methodology as in [17], one needs a change of variable that transform the second-order wave equations for n_j into a first-order system. We introduce this change of variable using the square root of the negative Laplacian, which is defined in the Fourier space. This multi-dimensional extension inherits all the properties of the one-dimensional scheme, as will be demonstrated by extensive numerical experiments. In particular, in the subsonic regime $0 < \epsilon \ll 1$, the asymptotic analysis and numerical examples indicate that the scheme converges uniformly with respect to ϵ for all the dispersive and nondispersive fields, for any initial data, upon a suitable initial layer fix by an L-stable time discretization.

The organization of this paper is as follows. In Sec. 2, we present the vectorial ZS for multi-component plasma and give a first-order

formulation of the second-order wave equations for nondispersive waves. In Sec. 3, we present our multidimensional TSSP method, and show asymptotically that it captures the correct subsonic limit numerically without resolving the small parameter ϵ_j. In Sec. 4, we present some numerical examples to verify the various properties and resolution capacity of the method. The paper concludes in Sec. 5.

2. EQUIVALENT FORM OF THE GENERALIZED ZS

Problems (1) and (2) must be supplemented with the initial conditions, say

$$\mathbf{E}(\mathbf{x}, 0) = \mathbf{E}_0(\mathbf{x}), \quad n_j(\mathbf{x}, 0) = n_{j,0}(\mathbf{x}), \quad n_{j,t}(\mathbf{x}, 0) = n_{j,1}(\mathbf{x}), \quad \forall j = 1, \ldots, \mathcal{J}. \tag{3}$$

From Eq. (2), we have

$$\int_{\mathcal{R}^d} n_{j,t}(\mathbf{x}, t)d\mathbf{x} = \int_{\mathcal{R}^d} n_{j,t}(\mathbf{x}, 0)d\mathbf{x} = \int_{\mathcal{R}^d} n_{j,1}(\mathbf{x})d\mathbf{x}, \quad \forall t, \quad \forall j. \tag{4}$$

Without loss of generality, we can assume

$$\int_{\mathcal{R}^d} n_{j,1}(\mathbf{x})d\mathbf{x} = 0. \tag{5}$$

Since if

$$\int_{\mathcal{R}^d} n_{j,1}(\mathbf{x})d\mathbf{x} = c_j \tag{6}$$

with c some fixed constant, the new unknown functions $\tilde{\mathbf{E}} = e^{-it^2/2\sum_{j=1}^{\mathcal{J}} c_j}\mathbf{E}$ and $\tilde{n}_j = n_j - c_j t$ satisfy the same Eqs. (1) and (2) as $\mathbf{E}$ and n_j, while

$$\int_{\mathcal{R}^d} \tilde{n}_{j,t}(\mathbf{x}, 0)d\mathbf{x} = \int_{\mathcal{R}^d} n_{j,1}(\mathbf{x})d\mathbf{x} - c_j = 0.$$

With the assumption (5), (4) implies

$$\int_{\mathcal{R}^d} n_{j,t}(\mathbf{x}, t)d\mathbf{x} = 0. \tag{7}$$

Equation (7) leads to the feasibility of introducing a new unknown function

$$v_j(x, t) \overset{\text{def}}{=} (-\Delta)^{-1/2} n_{j,t}(x, t). \tag{8}$$

Equation (8) is defined in the Fourier space by

$$\hat{v}_j(\mathbf{k}, t) = |\mathbf{k}|\hat{n}_{j,t}(\mathbf{k}, t). \tag{9}$$

Hereafter, for any function a defined in $\mathcal{R}^d$, we denote $\hat{a}$ as its *Fourier transform*, i.e.,

$$\hat{a}(\mathbf{k}) = \int_{\mathcal{R}^d_{\mathbf{x}}} a(\mathbf{x}) e^{-i\mathbf{k}\cdot\mathbf{x}} d\mathbf{x}. \tag{10}$$

It is well-known that a can be recovered from $\hat{a}$ by the *inverse Fourier transform*

$$a(\mathbf{x}) = \frac{1}{(2\pi)^d} \int_{\mathcal{R}^d_{\mathbf{k}}} \hat{a}(\mathbf{k}) e^{i\mathbf{x}\cdot\mathbf{k}} d\mathbf{k}. \tag{11}$$

Now systems (1) and (2) is equivalent to

$$i\mathbf{E}_t - \alpha\nabla\times(\nabla\times\mathbf{E}) + \nabla(\nabla\cdot\mathbf{E}) + \lambda|\mathbf{E}|^2\mathbf{E} + \textstyle\sum_{j=1}^{\mathcal{J}} n_j\mathbf{E} = 0, \tag{12}$$

$$n_{j,t} = (-\Delta)^{1/2} v_j, \tag{13}$$

$$\epsilon_j^2 v_{j,t} + (-\Delta)^{1/2}(n_j - \mu_j|\mathbf{E}|^2) = 0, \quad j = 1, \ldots, \mathcal{J} \tag{14}$$

with initial data

$$\mathbf{E}(\mathbf{x}, 0) = \mathbf{E}_0(\mathbf{x}), \quad n_j(\mathbf{x}, 0) = n_{j,0}(\mathbf{x}), \quad v_j(\mathbf{x}, 0) = v_{j,0}(\mathbf{x}) \stackrel{\text{def}}{=} (-\Delta)^{-1/2} n_{j,1}(x). \tag{15}$$

Remark 1. For the continuous problems (1) and (2), the wave energy $N = \int_{\mathcal{R}^d} |\mathbf{E}|^2 \, d\mathbf{x}$ and the Hamiltonian

$$H = \int_{\mathcal{R}^d} \left\{ \alpha|\nabla\times\mathbf{E}|^2 + |\nabla\cdot\mathbf{E}|^2 - \frac{\lambda}{2}|\mathbf{E}|^4 + \sum_{j=1}^{\mathcal{J}} \frac{1}{2\mu_j}|n_j|^2 + \sum_{j=1}^{\mathcal{J}} \frac{\epsilon_j^2}{2\mu_j}|v_j|^2 - \sum_{j=1}^{\mathcal{J}} n_j|\mathbf{E}|^2 \right\} d\mathbf{x}$$

are conserved.

Remark 2. Thus far, we take the dispersive field $\mathbf{E}$ as a vectorial unknown function. When $\alpha = 1$, Eq. (1) can be rewritten as

$$i\mathbf{E}_t + \Delta\mathbf{E} + \lambda|\mathbf{E}|^2\mathbf{E} + \sum_{j=1}^{\mathcal{J}} n_j\mathbf{E} = 0. \tag{16}$$

If $\mathbf{E}$ has only one component, for example in three-dimensions, $\mathbf{E} = (E, 0, 0)$, Eq. (16) is reduced to a scalar one

$$iE_t + \Delta E + \lambda |E|^2 E + \sum_{j=1}^{\mathcal{J}} n_j E = 0.$$

Then the wave energy is $N = \int_{\mathcal{R}^3} |E|^2 d\mathbf{x}$ and the Hamiltonian is

$$H = \int_{\mathcal{R}^3} \left\{ |\nabla E|^2 - \frac{\lambda}{2}|E|^4 + \sum_{j=1}^{\mathcal{J}} \frac{1}{2\mu_j}|n_j|^2 + \sum_{j=1}^{\mathcal{J}} \frac{\epsilon_j^2}{2\mu_j}|v_j|^2 - \sum_{j=1}^{\mathcal{J}} n_j |E|^2 \right\} d\mathbf{x}.$$

3. NUMERICAL METHODS

We consider the problems (1) and (2) in a most general form. All the following steps can be followed *without any difficulty* for some special forms of the generalized ZS, for example, the dispersive field is scalar, or the space dimension is only one.

3.1. A Time-Splitting Spectral Method

As usual for such problems, we use the time-splitting technique. Suppose Δt is the time step and $t_m = m\Delta t$. $\mathbf{E}^m(\mathbf{x})$, $n^m(\mathbf{x})$ and $v^m(\mathbf{x})$ are the respective approximate functions of $\mathbf{E}(\mathbf{x}, t)$, $n(\mathbf{x}, t)$ and $v(\mathbf{x}, t)$ at time $t = t_m$. We first solve Schrödinger-type equation

$$i\mathbf{E}_t - \alpha \nabla \times (\nabla \times \mathbf{E}) + \nabla(\nabla \cdot \mathbf{E}) = 0 \tag{17}$$

with initial data $\mathbf{E}(\mathbf{x}, t_m) = \mathbf{E}^m(\mathbf{x})$ in $[t_m, t_{m+1}]$ to get $\mathbf{E}^*(\mathbf{x}) = \mathbf{E}(\mathbf{x}, t_{m+1})$. Then we solve

$$i\mathbf{E}_t + \lambda |\mathbf{E}|^2 \mathbf{E} + \sum_{j=1}^{\mathcal{J}} n_j \mathbf{E} = 0, \tag{18}$$

$$n_{j,t} = (-\Delta)^{1/2} v_j, \tag{19}$$

$$\epsilon_j^2 v_{j,t} + (-\Delta)^{1/2}(n_j - \mu_j |\mathbf{E}|^2) = 0 \tag{20}$$

with initial data

$$\mathbf{E}(\mathbf{x}, t_m) = \mathbf{E}^*, \qquad n_j(\mathbf{x}, t_m) = n_j^m(\mathbf{x}), \qquad v_j(\mathbf{x}, t_m) = v_j^m(\mathbf{x})$$

again in $[t_m, t_{m+1}]$ to obtain

$$\mathbf{E}^{m+1}(\mathbf{x}) = \mathbf{E}(\mathbf{x}, t_{m+1}), \qquad n_j^{m+1}(\mathbf{x}) = n_j(\mathbf{x}, t_{m+1}), \qquad v_j^{m+1}(\mathbf{x}) = v_j(\mathbf{x}, t_{m+1}).$$

Now using Fourier transform with respect to spatial variable on (17), we obtain

$$i\hat{\mathbf{E}}_t - [\alpha|\mathbf{k}|^2\mathbf{I} + (1-\alpha)\mathbf{k}\otimes\mathbf{k}]\hat{\mathbf{E}} = 0. \tag{21}$$

Here, $\otimes$ is the tensor product operator. Thus we have

$$\hat{\mathbf{E}}^* = e^{-i\Delta t[\alpha|\mathbf{k}|^2\mathbf{I}+(1-\alpha)\mathbf{k}\otimes\mathbf{k}]}\hat{\mathbf{E}}^m. \tag{22}$$

A simple computation shows that

$$\begin{aligned} e^{-i\Delta t[\alpha|\mathbf{k}|^2\mathbf{I}+(1-\alpha)\mathbf{k}\otimes\mathbf{k}]} &= \left(\mathbf{I} - \frac{\mathbf{k}\otimes\mathbf{k}}{|\mathbf{k}|^2}\right)e^{-i\Delta t\alpha|\mathbf{k}|^2} + \frac{\mathbf{k}\otimes\mathbf{k}}{|\mathbf{k}|^2}e^{-i\Delta t|\mathbf{k}|^2} \\ &= e^{-i\Delta t\alpha|\mathbf{k}|^2}\mathbf{I} + \frac{\mathbf{k}\otimes\mathbf{k}}{|\mathbf{k}|^2}\left(e^{-i\Delta t|\mathbf{k}|^2} - e^{-i\Delta t\alpha|\mathbf{k}|^2}\right). \end{aligned} \tag{23}$$

From Eq. (18), it is easy to prove

$$\frac{d}{dt}|\mathbf{E}|^2 = 0, \qquad |\mathbf{E}(\mathbf{x}, t)|^2 = |\mathbf{E}(\mathbf{x}, t_m)|^2 = |\mathbf{E}^*(\mathbf{x})|^2.$$

Thus problems (18)–(20) is equivalent to

$$i\mathbf{E}_t + \lambda|\mathbf{E}^*|^2\mathbf{E} + \sum_{j=1}^{\mathcal{J}} n_j\mathbf{E} = 0, \tag{24}$$

$$n_{j,t} = (-\Delta)^{1/2}v_j, \tag{25}$$

$$\epsilon_j^2 v_{j,t} + (-\Delta)^{1/2}(n_j - \mu_j|\mathbf{E}^*|^2) = 0. \tag{26}$$

The most remarkable gain thus far is that with time-splitting technique, we decouple the dispersive field $\mathbf{E}$ and nondispersive field n_j. Let $w = |\mathbf{E}^*|^2$. We use Crank–Nicolson method to discretize the time derivatives in (25) and (26). In Fourier space, we have

$$\frac{\hat{n}_j^{m+1} - \hat{n}_j^m}{\Delta t} = \frac{|\mathbf{k}|}{2}(\hat{v}_j^{m+1} + \hat{v}_j^m), \tag{27}$$

$$\epsilon_j^2\frac{\hat{v}_j^{m+1} - \hat{v}_j^m}{\Delta t} + \frac{|\mathbf{k}|}{2}(\hat{n}_j^{m+1} + \hat{n}_j^m - 2\mu_j\hat{w}) = 0. \tag{28}$$

Equation (24) can be solved as

$$\mathbf{E}(\mathbf{x}, t) = e^{i\lambda(t-t_m)|\mathbf{E}^*(\mathbf{x})|^2} e^{i\int_{t_m}^{t} \sum_{j=1}^{\mathcal{J}} n_j(\mathbf{x},\tau)d\tau} \mathbf{E}^*(\mathbf{x}). \tag{29}$$

After n_j is solved, we can obtain $\mathbf{E}^{m+1}(\mathbf{x}) = \mathbf{E}(\mathbf{x}, t_{m+1})$ by approximating the integral in (29) with second-order trapezoidal quadrature rule:

$$\mathbf{w}_{1j} = \frac{4\epsilon_j^2 - |\mathbf{k}|^2\Delta t^2}{4\epsilon_j^2 + |\mathbf{k}|^2\Delta t^2}, \qquad \mathbf{w}_{2j} = \frac{4\epsilon_j|\mathbf{k}|\Delta t}{4\epsilon_j^2 + |\mathbf{k}|^2\Delta t^2}, \tag{30}$$

$$\hat{n}_j^{m+1} = \mathbf{w}_{1j}\hat{n}_j^m + \epsilon_j \mathbf{w}_{2j}\hat{v}_j^m + (1-\mathbf{w}_{1j})\mu_j\hat{w}, \tag{31}$$

$$\hat{v}_j^{m+1} = \mathbf{w}_{1j}\hat{v}_j^m - \frac{\mathbf{w}_{2j}}{\epsilon_j}\hat{n}_j^m + \frac{\mathbf{w}_{2j}}{\epsilon_j}\mu_j\hat{w}, \quad \forall j = 1, \ldots, \mathcal{J}, \tag{32}$$

$$\mathbf{E}^{m+1} = e^{i\Delta t\left[\lambda|\mathbf{E}^*|^2 + \frac{1}{2}\sum_{j=1}^{\mathcal{J}}(n_j^m + n_j^{m+1})\right]}\mathbf{E}^*. \tag{33}$$

Remark 3. We have an alternative to solve problems (25) and (26), i.e., we solve it in Fourier space *analytically*. That will lead to another numerical scheme, which can be used in many situations. Since its performance in the subsonic regime is inferior to the Crank–Nicolson methods (27) and (28) (see [17]), we do not elaborate on this scheme.

Up to now, we have only considered the approximation of time variable. To discretize the spatial derivatives, typically we need to confine our problem on a bounded domain and supplement some boundary conditions. Here we restrict to a cuboid domain with periodic boundary conditions. For other kind boundary conditions, one can consider replacing the Fourier method by a different approach such as the Chebeshev method [6].

Suppose $\mathcal{Q} = \Pi_{i=1}^{d}[-L_i, L_i]$ is the cuboid. Let even number M_i be the number of grid points in the ith direction. Denote

$$\mathcal{X} = \left\{ \left(\ldots, \frac{2L_i j_i}{M_i}, \ldots \right) \middle| 1 \leqslant i \leqslant d, -M_i/2 \leqslant j_i < M_i/2 \right\} \tag{34}$$

as the set of all grid points, and

$$\mathcal{K} = \left\{ \left(\ldots, \frac{\pi j_i}{L_i}, \ldots \right) \middle| 1 \leqslant i \leqslant d, -M_i/2 \leqslant j_i < M_i/2 \right\} \tag{35}$$

as the set of all discrete wave numbers. We define the *discrete Fourier transform* as

$$\hat{a}(\mathbf{k}) = \sum_{\mathbf{x}\in\mathcal{X}} a(\mathbf{x}) e^{-i\mathbf{k}\cdot\mathbf{x}}, \quad \forall \mathbf{k} \in \mathcal{K}, \tag{36}$$

where $a(\mathbf{x})$ can be recovered by the inverse discrete Fourier transform

$$a(\mathbf{x}) = \frac{1}{\Pi_{i=1}^{d} M_i} \sum_{\mathbf{k}\in\mathcal{K}} \hat{a}(\mathbf{k}) e^{i\mathbf{x}\cdot\mathbf{k}}, \quad \forall \mathbf{x} \in \mathcal{X}. \tag{37}$$

Notice that we have used symbol $\hat{}$ to represent both the continuous and discrete Fourier transforms. Now replacing the Fourier transforms with their discrete counterpart, and using Strang splitting idea [22] to have second-order accuracy in time, we get the final version of our TSSP:

$$\mathbf{w}_{1j} = \frac{4\epsilon_j^2 - |\mathbf{k}|^2 \Delta t^2}{4\epsilon_j^2 + |\mathbf{k}|^2 \Delta t^2}, \qquad \mathbf{w}_{2j} = \frac{4\epsilon_j |\mathbf{k}| \Delta t}{4\epsilon_j^2 + |\mathbf{k}|^2 \Delta t^2}, \tag{38}$$

$$\hat{\mathbf{E}}^* = e^{-\frac{i\Delta t}{2}[\alpha|\mathbf{k}|^2\mathbf{I} + (1-\alpha)\mathbf{k}\otimes\mathbf{k}]} \hat{\mathbf{E}}^m, \qquad w = |\mathbf{E}^*|^2, \tag{39}$$

$$\hat{n}_j^{m+1} = \mathbf{w}_{1j} \hat{n}_j^m + \epsilon_j \mathbf{w}_{2j} \hat{v}_j^m + (1 - \mathbf{w}_{1j}) \mu_j \hat{w}, \tag{40}$$

$$\hat{v}_j^{m+1} = \mathbf{w}_{1j} \hat{v}_j^m - \frac{\mathbf{w}_{2j}}{\epsilon_j} \hat{n}_j^m + \frac{\mathbf{w}_{2j}}{\epsilon_j} \mu_j \hat{w}, \quad \forall j = 1, \ldots, \mathcal{J}, \tag{41}$$

$$\mathbf{E}^{**} = e^{i\Delta t\left[\lambda|\mathbf{E}^*|^2 + \frac{1}{2}\sum_{j=1}^{\mathcal{J}}(n_j^m + n_j^{m+1})\right]} \mathbf{E}^*, \tag{42}$$

$$\mathbf{E}^{m+1} = e^{-\frac{i\Delta t}{2}[\alpha|\mathbf{k}|^2\mathbf{I} + (1-\alpha)\mathbf{k}\otimes\mathbf{k}]} \hat{\mathbf{E}}^{**}, \quad m = 0, 1, \ldots \tag{43}$$

The TSSP is an *unconditionally stable* scheme and it conserves the discrete l^2-norm of $\mathbf{E}$. Besides, it is easy to verify that this scheme is time reversible. Furthermore, if a constant is added to the initial value of the nondispersive field n_j, all approximations n_j^m are shifted by the same value. This leads to the occurrence of a phase factor in the approximations $\mathbf{E}^m$ of the dispersive field and leaves $|\mathbf{E}^m|^2$ unchanged, which means that TSSP is time transverse invariant.

Remark 4. Our numerical scheme can be easily generalized to some modified forms of ZS, for example, one can add a damped term in the Schrödinger-type equation (see [4]) and a dissipative term in the wave equation (see [14])

$$i\mathbf{E}_t - \alpha\nabla\times(\nabla\times\mathbf{E}) + \nabla(\nabla\cdot\mathbf{E}) + \lambda|\mathbf{E}|^2\mathbf{E} + \sum_{j=1}^{\mathcal{J}} n_j\mathbf{E} + i\gamma\mathbf{E} = 0,$$

$$\epsilon_j^2 n_{j,tt} - \Delta n_j + \mu_j \Delta|\mathbf{E}|^2 = \nu_j \Delta n_{j,t}, \quad \forall j = 1, \ldots, \mathcal{J}.$$

3.2. The Subsonic Regime

Formally, when $\epsilon_{\mathcal{J}} \to 0^+$, the multi-component vectorial ZS reduces to the same-type but one-component-less system

$$i\mathbf{E}_t - \alpha\nabla\times(\nabla\times\mathbf{E}) + \nabla(\nabla\cdot\mathbf{E}) + (\lambda+\mu_{\mathcal{J}})|\mathbf{E}|^2\mathbf{E} + \sum_{j=1}^{\mathcal{J}-1} n_j\mathbf{E} + \beta_{\mathcal{J}}\mathbf{E} = 0, \quad (44)$$

$$\epsilon_j^2 n_{j,tt} - \Delta n_j + \mu_j \Delta|\mathbf{E}|^2 = 0, \quad \forall j = 1, \ldots, \mathcal{J}-1, \quad (45)$$

$$n_{\mathcal{J}} = \mu_{\mathcal{J}}|\mathbf{E}|^2 + \beta_{\mathcal{J}}, \quad (46)$$

where

$$\begin{aligned}\beta_{\mathcal{J}} &= \frac{1}{\mathrm{mes}(\mathcal{D})}\int_{\mathcal{D}} (n_{\mathcal{J}}(\mathbf{x},t) - \mu_{\mathcal{J}}|\mathbf{E}(\mathbf{x},t)|^2)d\mathbf{x} \\ &= \frac{1}{\mathrm{mes}(\mathcal{D})}\int_{\mathcal{D}} (n_{\mathcal{J},0}(x) - \mu_{\mathcal{J}}|\mathbf{E}_0(x)|^2)dx. \end{aligned} \quad (47)$$

Here, $\mathcal{D}$ is the definition domain. The last equality comes from formula (7). Notice that for the problem defined on the whole space, one has $\beta_{\mathcal{J}} = 0$. This convergence is strong in $\mathbf{E}$ and $\{n_j\}_{j=1}^{\mathcal{J}-1}$, but generally only weak in $n_{\mathcal{J}}$. To obtain a strong convergence, one needs to impose the *compatibility condition*

$$n_{\mathcal{J},0}(x) - \mu_{\mathcal{J}}|\mathbf{E}_0(x)|^2 - \beta_J = O(\epsilon_{\mathcal{J}}) \quad (48)$$

for the initial data [21]. If this compatibility condition is not met by the initial data, $n_{\mathcal{J}}$ is oscillatory in time (but not in space). If this oscillation is not resolved, generally, only weak convergence can be anticipated [19, 23].

As was first done in [17], we now analyze the behavior of TSSP in the subsonic regime. Without loss of generality, assume $\epsilon_j (1 \leqslant j \leqslant \mathcal{J}-1)$ fixed, and $\epsilon_{\mathcal{J}} \to 0$. From formula (38), one sees that

$$\mathbf{w}_{1\mathcal{J}} = \begin{cases} 1, & \text{if } \mathbf{k} = 0, \\ -1, & \text{otherwise.} \end{cases} \qquad \mathbf{w}_{2\mathcal{J}} = 0.$$

Thus,

$$n_{\mathcal{J}}^{m+1} + n_{\mathcal{J}}^{m} = 2\mu|\mathbf{E}^*|^2 + 2\beta. \quad (49)$$

Applying this to (42) in TTSP, one sees that TSSP collapses to the TSSP for the reduced systems (44) and (44). Thus we obtained the numerical

convergence for $\mathbf{E}, n_1, \ldots, n_{\mathcal{J}-1}$ for any initial data. Namely, one can capture the correct solution of $\mathbf{E}, n_1, \ldots, n_{\mathcal{J}-1}$ with $\Delta x, \Delta t$ fixed, and $\epsilon_J \to 0$!

However, the convergence of $n_{\mathcal{J}}$ behaves differently. It has to do with the compatibility condition (48). If $n_{\mathcal{J}}^0 - \mu|\mathbf{E}^0|^2 - \beta = O(1)$, since in each step,

$$\mathbf{E}^m - \mathbf{E}^* = O(\Delta t), \quad \mathbf{E}^{m+1} - \mathbf{E}^* = O(\Delta t),$$

formula (49) implies

$$n_{\mathcal{J}}^{m+1} - \mu|\mathbf{E}^{m+1}|^2 - \beta = O(1).$$

Thus, if the initial data does not satisfy the compatibility condition (48), such an incompatibility will be preserved at all later time, preventing n_2 from converging to $\mu|\mathbf{E}|^2 + \beta$.

Since the error of $n_{\mathcal{J}}$ is mainly caused by the initial incompatibility, as was pointed out in [17], an L-stable ODE solver [11] can remove this error. Such phenomenon (initial layer discrepancy) has been studied for hyperbolic systems with stiff relaxation terms (see [5, 16]), where L-stable ODE solvers were used to eliminate the error introduced by under-resolution of the initial layer. For the ZS problem, one could either replace the Crank–Nicolson (which is not L-stable) method by a second-order L-stable ODE solver, or more simply, use an L-stable scheme (such as the backward Euler method) for the first time step. Here we take the second approach. Since we only use the first-order scheme for one time step, the overall accuracy in time remains second-order. Below for completeness we list the full scheme (called TSSP-m)

$$\mathbf{w}_{1j}^* = \frac{\epsilon_j^2}{\epsilon_j^2 + |\mathbf{k}|^2 \Delta t^2}, \qquad \mathbf{w}_{2j}^* = \frac{\epsilon_j |\mathbf{k}| \Delta t}{\epsilon_j^2 + |\mathbf{k}|^2 \Delta t^2},$$

$$\hat{\mathbf{E}}^* = e^{-i\Delta t[\alpha|\mathbf{k}|^2\mathbf{I} + (1-\alpha)\mathbf{k}\otimes\mathbf{k}]}\hat{\mathbf{E}}^0, \qquad w = |\mathbf{E}^*|^2,$$

$$\hat{n}_j^1 = \mathbf{w}_{1j}^* \hat{n}_j^0 + \epsilon_j \mathbf{w}_{2j}^* \hat{v}_j^0 + (1 - \mathbf{w}_{1j}^*)\mu_j \hat{w},$$

$$\hat{v}_j^1 = \mathbf{w}_{1j}^* \hat{v}_j^0 - \frac{\mathbf{w}_{2j}^*}{\epsilon_j}\hat{n}_j^0 + \frac{\mathbf{w}_{2j}^*}{\epsilon_j}\mu_j \hat{w}, \quad \forall j = 1, \ldots, \mathcal{J},$$

$$\mathbf{E}^1 = e^{i\Delta t(\lambda|\mathbf{E}^*|^2 + \sum_{j=1}^{\mathcal{J}} n_j^1)}\mathbf{E}^*,$$

$$\mathbf{w}_{1j} = \frac{4\epsilon_j^2 - |\mathbf{k}|^2\Delta t^2}{4\epsilon_j^2 + |\mathbf{k}|^2\Delta t^2}, \quad \mathbf{w}_{2j} = \frac{4\epsilon_j |\mathbf{k}| \Delta t}{4\epsilon_j^2 + |\mathbf{k}|^2\Delta t^2},$$

$$\hat{\mathbf{E}}^* = e^{-\frac{i\Delta t}{2}[\alpha|\mathbf{k}|^2\mathbf{I} + (1-\alpha)\mathbf{k}\otimes\mathbf{k}]}\hat{\mathbf{E}}^m, \quad w = |\mathbf{E}^*|^2,$$

$$\hat{n}_j^{m+1} = \mathbf{w}_{1j}\hat{n}_j^m + \epsilon_j \mathbf{w}_{2j}\hat{v}_j^m + (1-\mathbf{w}_{1j})\mu_j \hat{w},$$

$$\hat{v}_j^{m+1} = \mathbf{w}_{1j}\hat{v}_j^m - \frac{\mathbf{w}_{2j}}{\epsilon_j}\hat{n}_j^m + \frac{\mathbf{w}_{2j}}{\epsilon_j}\mu_j \hat{w}, \quad \forall j = 1, \ldots, \mathcal{J},$$

$$\mathbf{E}^{**} = e^{i\Delta t\left[\lambda|\mathbf{E}^*|^2 + \frac{1}{2}\sum_{j=1}^{\mathcal{J}}(n_j^m + n_j^{m+1})\right]}\mathbf{E}^*,$$

$$\mathbf{E}^{m+1} = e^{-\frac{i\Delta t}{2}[\alpha|\mathbf{k}|^2\mathbf{I} + (1-\alpha)\mathbf{k}\otimes\mathbf{k}]}\hat{\mathbf{E}}^{**}, \quad m = 1, \ldots$$

4. NUMERICAL EXAMPLES

In this section, we use numerical examples to verify various properties of TSSP.

Example 1. Accuracy of TSSP. We consider

$$iE_t + \Delta E + nE = 0, \tag{50}$$

$$n_{tt} - \Delta n + \Delta|E|^2 = 0, \tag{51}$$

$$E_0(x, y) = \cos^2\frac{\pi x}{8}\cos^2\frac{\pi y}{8}, \qquad n_0(x, y) = 0, \qquad n_1(x, y) = 0. \tag{52}$$

We confine this problem on a periodical cell $\mathcal{Q} = [-4, 4] \times [-4, 4]$. Tables I and II list the relative errors. The "exact" solution is taken to be the numerical solution when sufficiently small spatial step $h = 1/32$ and time step $\Delta t = 0.001$ are used. From Tables I and II, we observe that TSSP is really second-order in time and spectrally accurate in space.

Table I. TSSP Errors at Time $t = 1$ with $h = 1/32$

Time step Δt	1/10	1/20	1/40	1/80
$\frac{\|\|E-E_{h,\Delta t}\|\|_{L^2(\mathcal{Q})}}{\|\|E\|\|_{L^2(\mathcal{Q})}}$	$3.957e^{-4}$	$9.972e^{-5}$	$2.491e^{-5}$	$6.197e^{-6}$
$\frac{\|\|n-n_{h,\Delta t}\|\|_{L^2(\mathcal{Q})}}{\|\|n\|\|_{L^2(\mathcal{Q})}}$	$2.656e^{-3}$	$6.644e^{-4}$	$1.659e^{-4}$	$4.129e^{-5}$
$\frac{\|\|E\|^2-\|E_{h,\Delta t}\|^2\|\|_{L^1(\mathcal{Q})}}{\|\|E\|^2\|\|_{L^1(\mathcal{Q})}}$	$5.227e^{-4}$	$1.309e^{-4}$	$3.269e^{-5}$	$8.134e^{-6}$

Table II. TSSP Errors at Time $t=1$ with $\Delta t=0.001$

Spatial step h	1	1/2	1/4	1/8
$\frac{\|\|E-E_{h,\Delta t}\|\|_{L^2(\mathcal{Q})}}{\|\|E\|\|_{L^2(\mathcal{Q})}}$	$1.104e^{-4}$	$4.168e^{-9}$	$1.113e^{-13}$	$8.372e^{-14}$
$\frac{\|\|n-n_{h,\Delta t}\|\|_{L^2(\mathcal{Q})}}{\|\|n\|\|_{L^2(\mathcal{Q})}}$	$2.448e^{-4}$	$3.307e^{-8}$	$8.219e^{-14}$	$4.914e^{-14}$
$\frac{\|\|E\|^2-\|E_{h,\Delta t}\|^2\|\|_{L^1(\mathcal{Q})}}{\|\|E\|^2\|\|_{L^1(\mathcal{Q})}}$	$8.759e^{-5}$	$5.354e^{-9}$	$1.317e^{-13}$	$8.751e^{-14}$

Example 2. Convergence rate to the subsonic limit of the vectorial ZS. The test problem is

$$iE_t + E_{xx} + \lambda|E|^2E + (n_1+n_2)E = 0, \tag{53}$$

$$n_{1,tt} - n_{1,xx} + |E|^2_{xx} = 0, \tag{54}$$

$$\epsilon^2 n_{2,tt} - n_{2,xx} + \mu|E|^2_{xx} = 0, \tag{55}$$

$$E_0(x) = \cos^2\frac{\pi x}{8}, \qquad n_{1,0} = n_{1,1} = n_{2,1} = 0, \qquad n_{2,0} = \nu|E_0|^2. \tag{56}$$

When $\epsilon \to 0$, this system converges to (in different sense for different component)

$$iE_t + E_{xx} + (\lambda+\mu)|E|^2E + n_1E + \beta E = 0, \tag{57}$$

$$n_{1,tt} - n_{1,xx} + |E|^2_{xx} = 0, \tag{58}$$

$$E_0(x) = \cos^2\frac{\pi x}{8}, \qquad n_{1,0} = n_{1,1} = 0, \tag{59}$$

$$n_2 = \mu|E|^2 + \beta. \tag{60}$$

Here, $\beta = 3(\nu-\mu)/8$ is determined by (47). We let $\lambda = -1$ and $\mu = 1$. Table III lists the errors between the original problems (53)–(56) and its reduction (57)–(59). Since $\nu = \mu$, the initial compatibility condition is fulfilled, all components of the solution converge in a strong sense (more precisely, in $\mathcal{C}([0,1], L^2(\mathcal{Q}))$ for E, n_1, n_2 and in $\mathcal{C}([0,1], L^1(\mathcal{Q}))$ for $|E|^2$). Besides, our numerical results show that the convergences are second-order, i.e., $O(\epsilon^2)$, which has also been observed through the numerical example 2 in [3].

The story is very different when the initial compatibility condition is violated (see Table IV), when $\nu = 0 \neq \mu$. At a first glance, one might imprudently draw a conclusion that problems (53)–(56) still reduces to problems

Table III. Errors at Time $t=1$ When Compatibility Condition $\nu=\mu$ is Satisfied

ϵ	0.05	0.025	0.0125	0.00625
$\frac{\|\|E^0-E^\epsilon\|\|_{L^2(\mathcal{Q})}}{\|\|E^0\|\|_{L^2(\mathcal{Q})}}$	$4.002e^{-4}$	$9.973e^{-5}$	$2.490e^{-5}$	$6.223e^{-6}$
$\frac{\|\|n_1^0-n_1^\epsilon\|\|_{L^2(\mathcal{Q})}}{\|\|n_1^0\|\|_{L^2(\mathcal{Q})}}$	$1.865e^{-4}$	$4.788e^{-5}$	$1.205e^{-5}$	$3.018e^{-6}$
$\frac{\|\|n_2^0-n_2^\epsilon\|\|_{L^2(\mathcal{Q})}}{\|\|n_2^0\|\|_{L^2(\mathcal{Q})}}$	$1.564e^{-3}$	$1.699e^{-4}$	$4.238e^{-5}$	$1.059e^{-5}$
$\frac{\|\|\|E^0\|^2-\|E^\epsilon\|^2\|\|_{L^1(\mathcal{Q})}}{\|\|\|E^0\|^2\|\|_{L^1(\mathcal{Q})}}$	$1.843e^{-4}$	$4.683e^{-5}$	$1.166e^{-5}$	$2.912e^{-6}$

(E^0, n_1^0, n_2^0) Denotes the Solution of the reduction problems (57)–(59), while $(E^\epsilon, n_1^\epsilon, n_2^\epsilon)$ is denoted as the solution of (53)–(56). All the *exact* solutions are obtained by TSSP with sufficiently small spatial step $h(=1/8)$ and sufficiently small time step $\Delta t(=0.00001)$.

Table IV. Same Setting as that in Table III Except $\nu=0$

ϵ	0.05	0.025	0.0125	0.00625	0.006
$\frac{\|\|E^0-E^\epsilon\|\|_{L^2(\mathcal{Q})}}{\|\|E^0\|\|_{L^2(\mathcal{Q})}}$	$2.239e^{-3}$	$4.946e^{-4}$	$1.234e^{-4}$	$3.083e^{-5}$	$2.731e^{-3}$
$\frac{\|\|n_1^0-n_1^\epsilon\|\|_{L^2(\mathcal{Q})}}{\|\|n_1^0\|\|_{L^2(\mathcal{Q})}}$	$5.618e^{-3}$	$1.418e^{-3}$	$3.528e^{-4}$	$8.809e^{-5}$	$8.117e^{-5}$
$\frac{\|\|n_2^0-n_2^\epsilon\|\|_{L^2(\mathcal{Q})}}{\|\|n_2^0\|\|_{L^2(\mathcal{Q})}}$	1.163	1.162	1.162	1.162	$5.823e^{-1}$
$\frac{\|\|\|E^0\|^2-\|E^\epsilon\|^2\|\|_{L^1(\mathcal{Q})}}{\|\|\|E^0\|^2\|\|_{L^1(\mathcal{Q})}}$	$1.425e^{-3}$	$7.063e^{-4}$	$1.760e^{-4}$	$4.396e^{-5}$	$1.989e^{-5}$

Table V. Same Setting as that in Table III Except $\nu=0$

ϵ	$1/10\sqrt{5}$	$1/50$	$1/50\sqrt{5}$	$1/250$
$\frac{\|\|E^0-E^\epsilon\|\|_{L^2(\mathcal{Q})}}{\|\|E^0\|\|_{L^2(\mathcal{Q})}}$	$2.262e^{-2}$	$9.697e^{-3}$	$7.862e^{-4}$	$1.961e^{-3}$
$\frac{\|\|n_1^0-n_1^\epsilon\|\|_{L^2(\mathcal{Q})}}{\|\|n_1^0\|\|_{L^2(\mathcal{Q})}}$	$4.559e^{-3}$	$9.030e^{-4}$	$1.805e^{-4}$	$3.607e^{-5}$
$\frac{\|\|n_2^0-n_2^\epsilon\|\|_{L^2(\mathcal{Q})}}{\|\|n_2^0\|\|_{L^2(\mathcal{Q})}}$	$4.027e^{-1}$	$2.821e^{-1}$	1.147	$2.819e^{-1}$
$\frac{\|\|\|E^0\|^2-\|E^\epsilon\|^2\|\|_{L^1(\mathcal{Q})}}{\|\|\|E^0\|^2\|\|_{L^1(\mathcal{Q})}}$	$7.869e^{-4}$	$9.832e^{-5}$	$8.888e^{-5}$	$4.028e^{-6}$

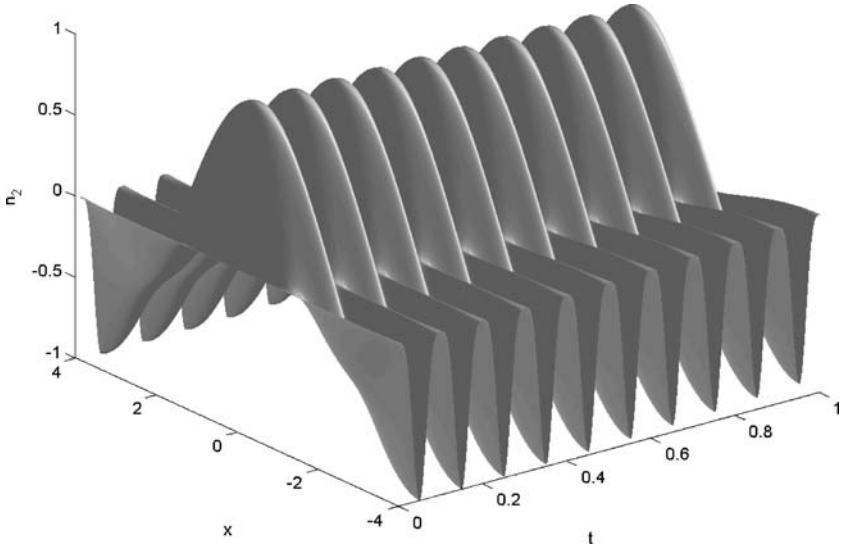

Fig. 1. Solution oscillatory in time. $\epsilon = 0.0125$.

(57)–(59) in the same rate, except n_2. But *this is not true*. First, the statistical results are highly sensitive with ϵ. A small change of ϵ results in a much different numerical results. See last column in Table IV (notice that n_0 converges truly in a second-order rate from our numerical experience). To make this point more clear, we list the numerical results for a different set of ϵ in Table V.

Why this happens is easy to explain. In fact, when the initial compatibility condition is violated, n_2 cannot be expected to converge in a strong sense, since it oscillates in time (see Fig. 1). It only converges in weak$-^*$ in $L^\infty(R^+, L^2(\mathcal{Q}))$, i.e., for any $\psi \in L^1(R^+, L^2(\mathcal{Q}))$

$$< n_2^\epsilon - n_2^0, \psi >_{L^1(R^+, L^2(\mathcal{Q}))} \to 0, \quad \text{when } \epsilon \to 0.$$

Besides, though E still strongly converges to its limitation, this holds in $L^2_{\text{loc}}(R^+, L^2(\mathcal{Q}))$, not in $\mathcal{C}([0, 1], L^2(\mathcal{Q}))$.

Table VI shows the results for different statistics. We see that E and $|E|^2$ converge with first-order, respectively, in $L^2_{\text{loc}}(R^+, L^2(\mathcal{Q}))$ and $L^1_{\text{loc}}(R^+, L^2(\mathcal{Q}))$, n_2 converges with second-order in weak$-^* L^\infty(R^+, L^2(\mathcal{Q}))$, but n_1 converges with second-order in a much stronger sense, $\mathcal{C}([0, 1], L^2(\mathcal{Q}))$.

Example 3. Behavior of TSSP in the subsonic regime. The test problem is

$$iE_t + \Delta E + \lambda|E|^2E + (n_1 + n_2)E = 0, \tag{61}$$

$$n_{1,tt} - \Delta n_1 + \Delta|E|^2 = 0, \tag{62}$$

$$\epsilon^2 n_{2,tt} - \Delta n_2 + \mu\Delta|E|^2 = 0, \tag{63}$$

$$E_0(x, y) = \cos^2\tfrac{\pi x}{8}\cos^2\tfrac{\pi y}{8}, \qquad n_{1,0} = n_{1,1} = n_{2,1} = 0, \qquad n_{2,0} = \nu|E_0|^2, \tag{64}$$

when $\epsilon \to 0$, the solution converges to the solution of

$$iE_t + \Delta E + (\lambda + \mu)|E|^2E + n_1E + \beta E = 0, \tag{65}$$

$$n_{1,tt} - \Delta n_1 + \Delta|E|^2 = 0, \tag{66}$$

$$E_0(x, y) = \cos^2\frac{\pi x}{8}\cos^2\frac{\pi y}{8}, \qquad n_{1,0} = n_{1,1} = 0, \tag{67}$$

$$n_2 = \mu|E|^2 + \beta, \tag{68}$$

where $\beta = 9(\nu - \mu)/64$ is determined by (47). We use this problem to test the numerical performance of TSSP in the whole regime $0 < \epsilon < 1$. Typically, we choose three values in different scales, $\epsilon_1 = 1$, $\epsilon_2 = 10^{-2}$ and $\epsilon_2 = 10^{-4}$. The "exact" solutions $(E^{\epsilon_1}, n_1^{\epsilon_1}, n_2^{\epsilon_1})$ and $(E^{\epsilon_2}, n_1^{\epsilon_2}, n_2^{\epsilon_2})$ are approximated by TSSP with sufficiently small spatial step and sufficiently small time step. Since ϵ_3 is too small and difficult to resolve numerically in our computing capacity, we replace $(E^{\epsilon_3}, n_1^{\epsilon_3}, n_2^{\epsilon_3})$ by (E^0, n_1^0, n_2^0), when $\nu = \mu$, and $n_1^{\epsilon_3} = n_1^0$, when $\nu = 0$, due to their strong second-order convergence when $\epsilon \to 0$.

Tables VII–IX list the errors for different ϵ, when $\nu = \mu$. The results show that the solution converges, as the time step goes to zero, uniformly in ϵ, for *all* components.

Tables X–XIII list the errors for ϵ_1 and ϵ_2 when $\nu = 0 \neq \mu$. We see that generally, we cannot get a convergence for n_2 if the time scale is not small enough compared to ϵ. However, we still get good approximation of **E** and n_1.

Tables XIV and XV list the errors when TSSP-m is used. We can see a second-order convergence in the subsonic regime $0 < \epsilon \ll 1$ for all quantities, even the initial compatibility condition is not met.

These numerical experiments confirm our asymptotic analysis in the subsonic regime carried out in Sec. 3.2.

Example 4. Blow-up problem and Conservation of Hamiltonian. The test problem is a two-dimensional scalar problem with one ion species

Table VI. Same Setting as that in Table III Except $\nu = 0$. We Let $\psi(x,t) = e^{\sin \pi x/4}$

ϵ	0.05	0.025	0.0125	0.00625
$\frac{\|\|E^0 - E^\epsilon\|\|_{L^2([0,1]\times\mathcal{Q})}}{\|\|E^0\|\|_{L^2([0,1]\times\mathcal{Q})}}$	$1.742e^{-2}$	$8.704e^{-3}$	$4.341e^{-3}$	$2.169e^{-3}$
$\frac{\|\|n_1^0 - n_1^\epsilon\|\|_{L^2(\mathcal{Q})}}{\|\|n_1^0\|\|_{L^2(\mathcal{Q})}}\Big\|_{t=1}$	$5.618e^{-3}$	$1.418e^{-3}$	$3.528e^{-4}$	$8.809e^{-5}$
$< n_2^0 - n_2^\epsilon, \psi >_{L^1([0,1],L^2(\mathcal{Q}))}$	$-4.127e^{-4}$	$-1.020e^{-4}$	$-2.548e^{-5}$	$-6.337e^{-6}$
$\frac{\|\|\|E^0\|^2 - \|E^\epsilon\|^2\|\|_{L^2([0,1]\times\mathcal{Q})}}{\|\|\|E^0\|^2\|\|_{L^2([0,1]\times\mathcal{Q})}}$	$4.399e^{-2}$	$2.197e^{-2}$	$1.097e^{-2}$	$5.482e^{-3}$

Table VII. $\epsilon = 1,\ \nu = \mu$

Time step Δt	1/25	1/50	1/100	1/200	1/400
$\frac{\|\|E^\epsilon - E^\epsilon_{\Delta t}\|\|_{L^2(\mathcal{Q})}}{\|\|E^\epsilon\|\|_{L^2(\mathcal{Q})}}$	$6.202e^{-5}$	$1.551e^{-5}$	$3.877e^{-6}$	$9.688e^{-7}$	$2.419e^{-7}$
$\frac{\|\|n_1^\epsilon - n_{1\Delta t}^\epsilon\|\|_{L^2(\mathcal{Q})}}{\|\|n_1^\epsilon\|\|_{L^2(\mathcal{Q})}}$	$4.286e^{-4}$	$1.072e^{-4}$	$2.679e^{-5}$	$6.696e^{-6}$	$1.672e^{-6}$
$\frac{\|\|n_2^\epsilon - n_{2\Delta t}^\epsilon\|\|_{L^2(\mathcal{Q})}}{\|\|n_2^\epsilon\|\|_{L^2(\mathcal{Q})}}$	$2.085e^{-5}$	$5.202e^{-6}$	$1.300e^{-6}$	$3.248e^{-7}$	$8.110e^{-8}$
$\frac{\|\|\|E^\epsilon\|^2 - \|E^\epsilon_{\Delta t}\|^2\|\|_{L^1(\mathcal{Q})}}{\|\|\|E^\epsilon\|^2\|\|_{L^1(\mathcal{Q})}}$	$9.481e^{-5}$	$2.370e^{-5}$	$5.926e^{-6}$	$1.481e^{-6}$	$3.698e^{-7}$

Table VIII. $\epsilon = 10^{-2},\ \nu = \mu$

Time step Δt	1/25	1/50	1/100	1/200	1/400
$\frac{\|\|E^\epsilon - E^\epsilon_{\Delta t}\|\|_{L^2(\mathcal{Q})}}{\|\|E^\epsilon\|\|_{L^2(\mathcal{Q})}}$	$6.389e^{-5}$	$1.599e^{-5}$	$4.022e^{-6}$	$1.015e^{-6}$	$2.535e^{-7}$
$\frac{\|\|n_1^\epsilon - n_{1\Delta t}^\epsilon\|\|_{L^2(\mathcal{Q})}}{\|\|n_1^\epsilon\|\|_{L^2(\mathcal{Q})}}$	$4.254e^{-4}$	$1.063e^{-4}$	$2.659e^{-5}$	$6.646e^{-6}$	$1.660e^{-6}$
$\frac{\|\|n_2^\epsilon - n_{2\Delta t}^\epsilon\|\|_{L^2(\mathcal{Q})}}{\|\|n_2^\epsilon\|\|_{L^2(\mathcal{Q})}}$	$2.029e^{-4}$	$3.559e^{-5}$	$9.186e^{-5}$	$2.458e^{-5}$	$1.292e^{-5}$
$\frac{\|\|\|E^\epsilon\|^2 - \|E^\epsilon_{\Delta t}\|^2\|\|_{L^1(\mathcal{Q})}}{\|\|\|E^\epsilon\|^2\|\|_{L^1(\mathcal{Q})}}$	$8.382e^{-5}$	$2.096e^{-5}$	$5.245e^{-6}$	$1.311e^{-6}$	$3.261e^{-7}$

$$iE_t + \Delta E + nE = 0, \tag{69}$$

$$n_{tt} - \Delta n + \mu \Delta |E|^2 = 0. \tag{70}$$

The initial conditions are set to be

$$E_0(x,y) = \frac{1}{\sqrt{\pi}} e^{-\frac{x^2+y^2}{2}}, \qquad n_0(x,y) = \nu |E_0(x,y)|^2, \qquad n_1(x,y) = 0. \tag{71}$$

Table IX. $\epsilon = 10^{-4},\ \nu = \mu$

Time step Δt	1/25	1/50	1/100	1/200	1/400
$\frac{\|\|E^\epsilon - E^\epsilon_{\Delta t}\|\|_{L^2(\mathcal{Q})}}{\|\|E^\epsilon\|\|_{L^2(\mathcal{Q})}}$	$6.385e^{-5}$	$1.597e^{-5}$	$3.991e^{-6}$	$9.971e^{-7}$	$2.487e^{-7}$
$\frac{\|\|n_1^\epsilon - n_{1\Delta t}^\epsilon\|\|_{L^2(\mathcal{Q})}}{\|\|n_1^\epsilon\|\|_{L^2(\mathcal{Q})}}$	$4.252e^{-4}$	$1.064e^{-4}$	$2.660e^{-5}$	$6.649e^{-6}$	$1.662e^{-6}$
$\frac{\|\|n_2^\epsilon - n_{2\Delta t}^\epsilon\|\|_{L^2(\mathcal{Q})}}{\|\|n_2^\epsilon\|\|_{L^2(\mathcal{Q})}}$	$1.604e^{-4}$	$3.789e^{-5}$	$8.749e^{-6}$	$2.065e^{-6}$	$5.724e^{-7}$
$\frac{\|\|\|E^\epsilon\|^2 - \|E^\epsilon_{\Delta t}\|^2\|\|_{L^1(\mathcal{Q})}}{\|\|\|E^\epsilon\|^2\|\|_{L^1(\mathcal{Q})}}$	$8.380e^{-5}$	$2.095e^{-5}$	$5.238e^{-6}$	$1.308e^{-6}$	$3.259e^{-7}$

Table X. $\epsilon = 1,\ \nu = 0$

Time step Δt	1/25	1/50	1/100	1/200	1/400
$\frac{\|\|E^\epsilon - E^\epsilon_{\Delta t}\|\|_{L^2(\mathcal{Q})}}{\|\|E^\epsilon\|\|_{L^2(\mathcal{Q})}}$	$6.476e^{-5}$	$1.618e^{-5}$	$4.045e^{-6}$	$1.011e^{-6}$	$2.524e^{-7}$
$\frac{\|\|n_1^\epsilon - n_{1\Delta t}^\epsilon\|\|_{L^2(\mathcal{Q})}}{\|\|n_1^\epsilon\|\|_{L^2(\mathcal{Q})}}$	$3.355e^{-4}$	$8.388e^{-5}$	$2.097e^{-5}$	$5.241e^{-6}$	$1.309e^{-6}$
$\frac{\|\|n_2^\epsilon - n_{2\Delta t}^\epsilon\|\|_{L^2(\mathcal{Q})}}{\|\|n_2^\epsilon\|\|_{L^2(\mathcal{Q})}}$	$3.355e^{-4}$	$8.388e^{-5}$	$2.097e^{-5}$	$5.241e^{-6}$	$1.309e^{-6}$
$\frac{\|\|\|E^\epsilon\|^2 - \|E^\epsilon_{\Delta t}\|^2\|\|_{L^1(\mathcal{Q})}}{\|\|\|E^\epsilon\|^2\|\|_{L^1(\mathcal{Q})}}$	$8.171e^{-5}$	$2.041e^{-5}$	$5.102e^{-6}$	$1.275e^{-6}$	$3.184e^{-7}$

Table XI. $\epsilon = 10^{-2},\ \nu = 0$

Time step Δt	1/25	1/50	1/100	1/200	1/400
$\frac{\|\|E^\epsilon - E^\epsilon_{\Delta t}\|\|_{L^2(\mathcal{Q})}}{\|\|E^\epsilon\|\|_{L^2(\mathcal{Q})}}$	$2.172e^{-3}$	$1.060e^{-3}$	$1.215e^{-3}$	$4.728e^{-3}$	$1.241e^{-3}$
$\frac{\|\|n_1^\epsilon - n_{1\Delta t}^\epsilon\|\|_{L^2(\mathcal{Q})}}{\|\|n_1^\epsilon\|\|_{L^2(\mathcal{Q})}}$	$4.258e^{-4}$	$1.064e^{-4}$	$2.670e^{-5}$	$6.667e^{-6}$	$1.647e^{-6}$
$\frac{\|\|n_2^\epsilon - n_{2\Delta t}^\epsilon\|\|_{L^2(\mathcal{Q})}}{\|\|n_2^\epsilon\|\|_{L^2(\mathcal{Q})}}$	1.073	$1.273e^{-1}$	$9.988e^{-1}$	$3.207e^{-1}$	$3.206e^{-1}$
$\frac{\|\|\|E^\epsilon\|^2 - \|E^\epsilon_{\Delta t}\|^2\|\|_{L^1(\mathcal{Q})}}{\|\|\|E^\epsilon\|^2\|\|_{L^1(\mathcal{Q})}}$	$1.760e^{-4}$	$1.973e^{-5}$	$9.752e^{-5}$	$1.848e^{-5}$	$3.822e^{-5}$

Theoretically, if $H = 1 + \frac{\nu^2/\mu - 2\nu}{4\pi} < 0$, i.e., $2\nu - \nu^2/\mu > 4\pi$, the solution of this system will blow up at some time. When $\mu = 20$ and $\nu = 20$, $H \approx -0.5915 < 0$. Figures 2–7 show the numerical solutions at different time points. One can see that a singularity indeed starts to form as time evolves. Table XVI lists the numerical Hamiltonians for different ν at different time points, when $\mu = 20$. One can observe that TSSP conserves the Hamiltonian very well (one might notice that at $t = 1.0$ when $\nu = 20$, the result differs a little much. This can be taken as a numerical artifact since the

Table XII. $\epsilon = 10^{-4},\ \nu = 0$

Time step Δt	1/25	1/50	1/100	1/200	1/400
$\frac{\|\|E^0 - E^\epsilon_{\Delta t}\|\|_{L^2(\mathcal{Q})}}{\|\|E^0\|\|_{L^2(\mathcal{Q})}}$	$6.345e^{-5}$	$4.535e^{-5}$	$3.089e^{-5}$	$4.085e^{-5}$	$8.023e^{-6}$
$\frac{\|\|n_1^0 - n^\epsilon_{1\Delta t}\|\|_{L^2(\mathcal{Q})}}{\|\|n_1^0\|\|_{L^2(\mathcal{Q})}}$	$4.255e^{-4}$	$1.064e^{-4}$	$2.661e^{-5}$	$6.662e^{-6}$	$1.675e^{-6}$
$\frac{\|\|n_2^0 - n^\epsilon_{2\Delta t}\|\|_{L^2(\mathcal{Q})}}{\|\|n_2^0\|\|_{L^2(\mathcal{Q})}}$	1.161	$5.604e^{-1}$	$5.905e^{-1}$	$3.129e^{-1}$	$9.178e^{-1}$
$\frac{\|\|\|E^0\|^2 - \|E^\epsilon_{\Delta t}\|^2\|\|_{L^1(\mathcal{Q})}}{\|\|\|E^0\|^2\|\|_{L^1(\mathcal{Q})}}$	$8.379e^{-5}$	$2.096e^{-5}$	$5.236e^{-6}$	$1.307e^{-6}$	$3.305e^{-7}$

Table XIII. $\epsilon = 10^{-8},\ \nu = 0$

Time step Δt	1/25	1/50	1/100	1/200	1/400
$\frac{\|\|E^0 - E^\epsilon_{\Delta t}\|\|_{L^2(\mathcal{Q})}}{\|\|E^0\|\|_{L^2(\mathcal{Q})}}$	$6.385e^{-5}$	$1.596e^{-5}$	$3.990e^{-6}$	$9.963e^{-7}$	$2.478e^{-7}$
$\frac{\|\|n_1^0 - n^\epsilon_{1\Delta t}\|\|_{L^2(\mathcal{Q})}}{\|\|n_1^0\|\|_{L^2(\mathcal{Q})}}$	$4.254e^{-4}$	$1.064e^{-4}$	$2.660e^{-5}$	$6.649e^{-6}$	$1.663e^{-6}$
$\frac{\|\|n_2^0 - n^\epsilon_{2\Delta t}\|\|_{L^2(\mathcal{Q})}}{\|\|n_2^0\|\|_{L^2(\mathcal{Q})}}$	1.209	1.209	1.209	1.209	1.209
$\frac{\|\|\|E^0\|^2 - \|E^\epsilon_{\Delta t}\|^2\|\|_{L^1(\mathcal{Q})}}{\|\|\|E^0\|^2\|\|_{L^1(\mathcal{Q})}}$	$8.380e^{-5}$	$2.095e^{-5}$	$5.237e^{-6}$	$1.308e^{-6}$	$3.252e^{-7}$

Table XIV. $\epsilon = 10^{-4}$, TSSP-m is Used

Time step Δt	1/25	1/50	1/100	1/200	1/400
$\frac{\|\|E^0 - E^\epsilon\|\|_{L^2(\mathcal{Q})}}{\|\|E^0\|\|_{L^2(\mathcal{Q})}}$	$3.637e^{-4}$	$9.088e^{-5}$	$2.272e^{-5}$	$5.716e^{-6}$	$2.752e^{-6}$
$\frac{\|\|n_1^0 - n_1^\epsilon\|\|_{L^2(\mathcal{Q})}}{\|\|n_1^0\|\|_{L^2(\mathcal{Q})}}$	$6.180e^{-4}$	$1.570e^{-4}$	$3.957e^{-5}$	$9.931e^{-6}$	$2.485e^{-6}$
$\frac{\|\|n_2^0 - n_2^\epsilon\|\|_{L^2(\mathcal{Q})}}{\|\|n_2^0\|\|_{L^2(\mathcal{Q})}}$	$8.030e^{-4}$	$6.253e^{-3}$	$1.113e^{-2}$	$2.623e^{-2}$	$2.516e^{-2}$
$\frac{\|\|\|E^0\|^2 - \|E^\epsilon\|^2\|\|_{L^1(\mathcal{Q})}}{\|\|\|E^0\|^2\|\|_{L^1(\mathcal{Q})}}$	$3.662e^{-4}$	$9.148e^{-5}$	$2.286e^{-5}$	$5.712e^{-6}$	$1.427e^{-6}$

solution becomes much singular at this time, see Figs. 2–7). We note that this example has been utilized in [3] to demonstrate their numerical behavior.

Table XV. $\epsilon = 10^{-8}$, TSSP-m is Used

Time step Δt	1/25	1/50	1/100	1/200	1/400
$\frac{\|\|E^0 - E^\epsilon\|\|_{L^2(\mathcal{Q})}}{\|\|E^0\|\|_{L^2(\mathcal{Q})}}$	$3.638e^{-4}$	$9.080e^{-5}$	$2.268e^{-5}$	$5.666e^{-6}$	$1.414e^{-6}$
$\frac{\|\|n_1^0 - n_1^\epsilon\|\|_{L^2(\mathcal{Q})}}{\|\|n_1^0\|\|_{L^2(\mathcal{Q})}}$	$6.180e^{-4}$	$1.570e^{-4}$	$3.957e^{-5}$	$9.931e^{-6}$	$2.485e^{-6}$
$\frac{\|\|n_2^0 - n_2^\epsilon\|\|_{L^2(\mathcal{Q})}}{\|\|n_2^0\|\|_{L^2(\mathcal{Q})}}$	$2.174e^{-4}$	$1.074e^{-4}$	$2.683e^{-5}$	$6.706e^{-6}$	$1.707e^{-6}$
$\frac{\|\|\|E^0\|^2 - \|E^\epsilon\|^2\|\|_{L^1(\mathcal{Q})}}{\|\|\|E^0\|^2\|\|_{L^1(\mathcal{Q})}}$	$3.662e^{-4}$	$9.148e^{-5}$	$2.286e^{-5}$	$5.711e^{-6}$	$1.426e^{-6}$

Table XVI. Hamiltonians at Different Time Points Under $\mu = 20$.

	$t = 0.2$	$t = 0.4$	$t = 0.6$	$t = 0.8$	$t = 1.0$
$\nu = 5$	4.1831	4.1831	4.1831	4.1831	4.1831
$\nu = 10$	1.0000	1.0000	1.0000	1.0000	1.0000
$\nu = 20$	−0.5915	−0.5916	−0.5916	−0.5917	−0.5986

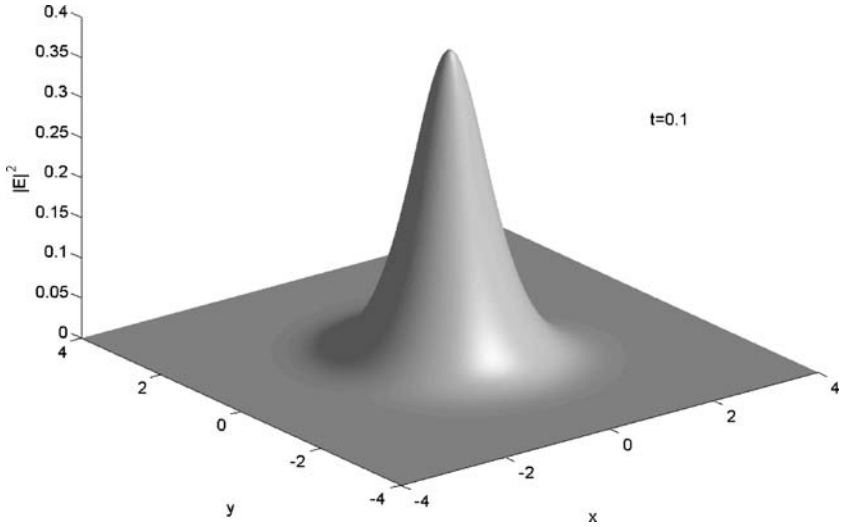

Fig. 2. Plot of energy density $|E|^2$ at time $t = 0.1$ in Example 4. $\mu = \nu = 20$.

5. CONCLUSION

A time-splitting spectral scheme TSSP has been proposed for generalized ZS in multi-dimensions. This scheme is unconditionally stable, sec-

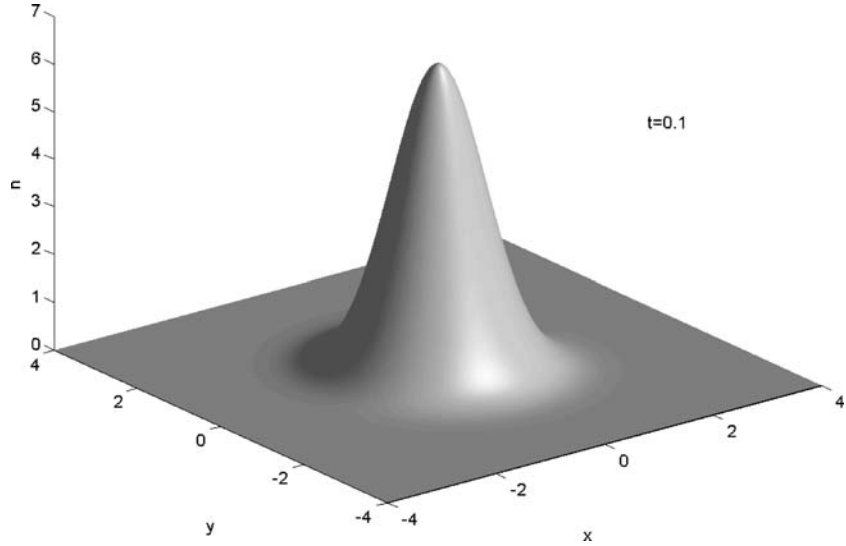

Fig. 3. Plot of ion density fluctuation n at time $t=0.1$ in Example 4. $\mu=\nu=20$.

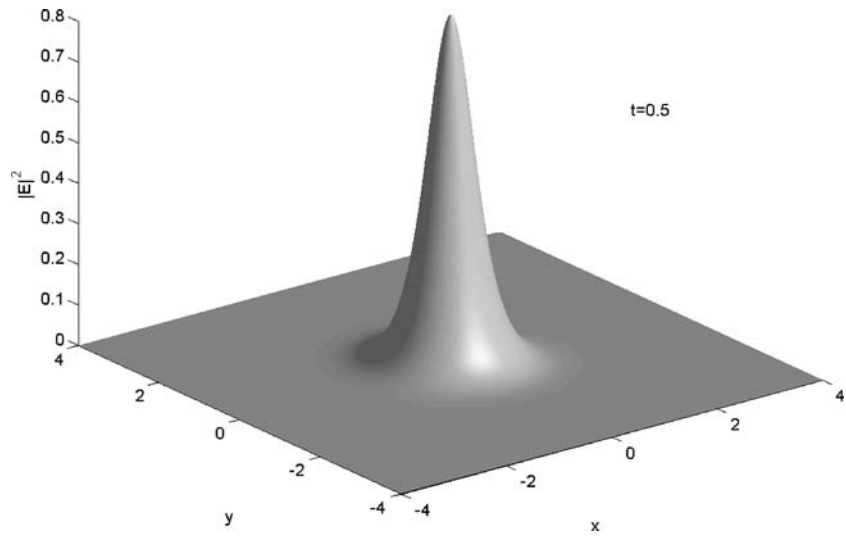

Fig. 4. Plot of energy density $|E|^2$ at time $t=0.5$ in Example 4. $\mu=\nu=20$.

ond-order in time and spectral order in space. Asymptotic analysis shows that the method is capable of capturing the correct solutions in the subsonic regimes without numerically resolving the subsonic parameters. A spread of numerical examples demonstrate the stated properties of TSSP.

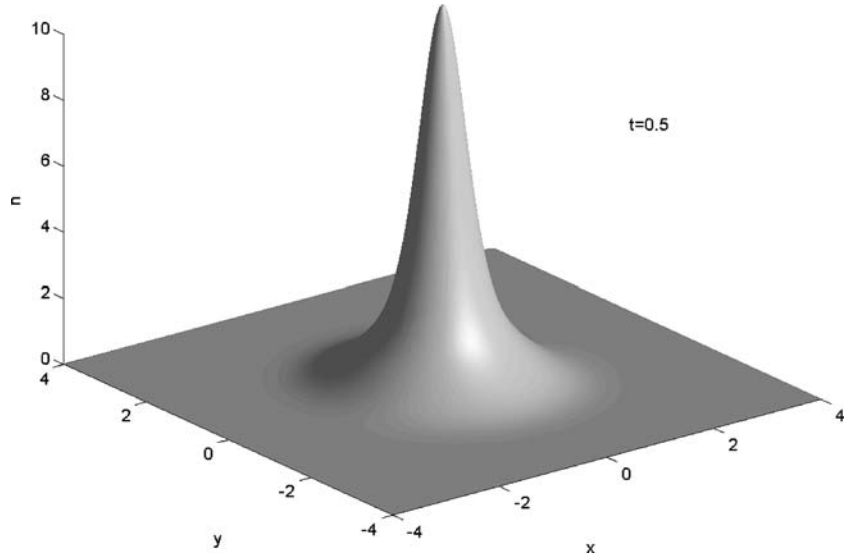

Fig. 5. Plot of ion density fluctuation n at time $t = 0.5$ in Example 4. $\mu = \nu = 20$.

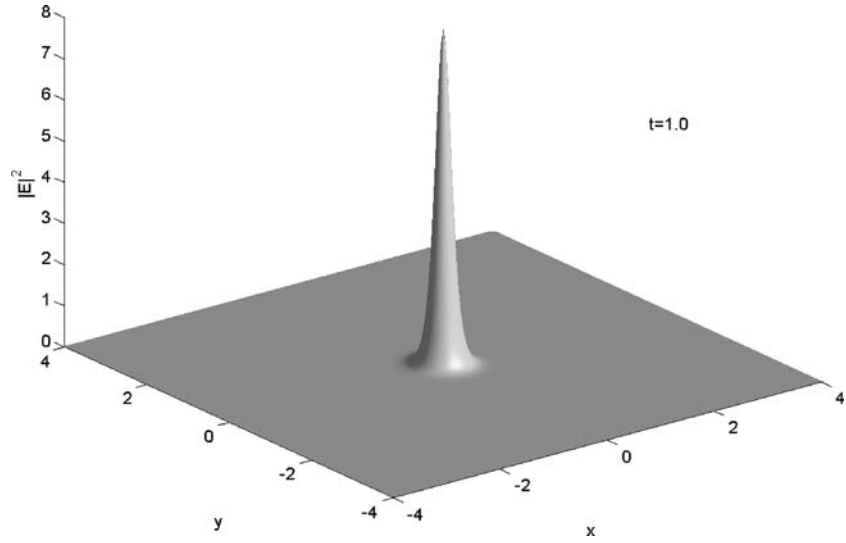

Fig. 6. Plot of energy density $|E|^2$ at time $t = 1.0$ in Example 4. $\mu = \nu = 20$.

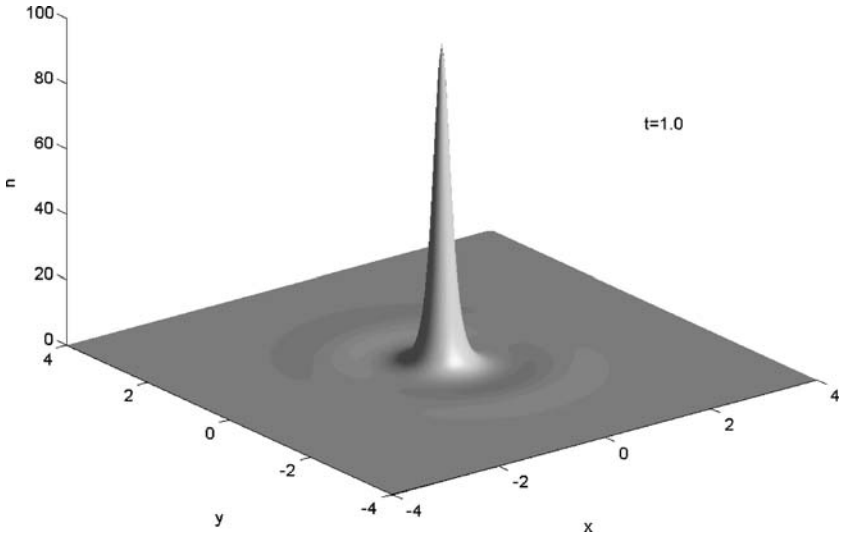

Fig. 7. Plot of ion density fluctuation n at time $t = 1.0$ in Example 4. $\mu = \nu = 20$.

ACKNOWLEDGMENTS

Research supported in part by U.S. National Science Foundation grant No. DMS-0305080, National Natural Science Foundation of China Project 10228101 and Project 10401020, and the Basic Research Projects of Tsinghua University under the Project JC2002010.

REFERENCES

1. Bao, W., Jin, S., and Markowich, P. A. (2002). On time-splitting spectral approximations for the Schrödinger equation in the semiclassical regime. *J. Comput. Phys.* **175**, 487–524.
2. Bao, W., Jin, S., and Markowich, P. A. (2003). Numerical study of time-splitting spectral discretizations of nonlinear Schrödinger equations in the semi-classical regimes. *SIAM J. Sci. Comp.* **25**, 27–64.
3. Bao, W., and Sun, F. F. (2005). Efficient and stable numerical methods for the generalized and vector Zakharov system. *SIAM J. Sci. Comput.* **26**(3), 1057–1088.
4. Bao, W., Sun, F. F., and Wei, G. W. (2003). Numerical methods for the generalized Zakharov system. *J. Comp. Phys.* **190**, 201–228.
5. Caflisch, R., Jin, S., and Russo, G. (1997). Uniformly accurate schemes for hyperbolic systems with relaxations. *SIAM J. Num. Anal.* **34,** 246–281.
6. Canuto, C., Hussaini, M. Y., Quarteroni, A., and Zang, T. A. (1988). *Spectral Methods in Fluid Dynamics*, Springer-Verlag, New York.
7. Chang, Q., and Jiang, H. (1994). A conservative difference scheme for the Zakharov equations. *J. Comput. Phys.* **113**(2), 309–319.

8. Chang, Q., Guo, B., and Jiang, H. (1995). Finite difference method for generalized Zakharov equations. *Math. Comp.* **64**, 537–553.
9. Davydov, A. S. (1979). Solitons in molecular systems. *Physica Scripta,* **20,** 387–394.
10. Degtyarev, L. M., Nakhan'kov, V. G., and Rudakov, L. I. (1974). Dynamics of the formation and interaction of Langmuir solitons and strong turbulence. *Sov. Phys. JETP* **40,** 264–268.
11. Gear, C. W. (1971). *Numerical Initial value Problems in Ordinary Differential Equations,* Prentice-Hall, Englewood Cliffs, NJ.
12. Glassey, R. (1992). Approximate solutions to the Zakharov equations via finite differences. *J. Comput. Phys.* **100,** 377–383.
13. Glassey, R. (1992). Convergence of an energy-preserving scheme for the Zakharov equations in one space dimension. *Math. Comp.* **58,** 83–102.
14. Hadouaj, H., Malomed, B. A., and Maugin, G. A. (1991). Dynamics of a soliton in a generalized Zakharov system with dissipation. *Phys. Rev. A,* **44**(6), 3925–3931.
15. Hadouaj, H., Malomed, B. A., and Maugin, G. A. (1991). Soliton-soliton collisions in a generalized Zakharov system. *Phys. Rev. A* **44**(6), 3932–3940.
16. Jin, S. (1995). Runge-Kutta methods for hyperbolic conservation laws with stiff relaxation terms. *J. Comp. Phys.* **122,** 51–67.
17. Jin, S., Markowich, P. A., and Zheng, C. X. (2004). Numerical simulation of a generalized Zakharov system, *J. Comput. Phys.* **201**(1), 376–395.
18. Pathria, D., and Morris, J. L. (1980). Pseudo-spectral solution of nonlinear Schrödinger equation. *J. Comput. Phys.* **87,** 108–125.
19. Ozawa, T., and Tsutsumi, Y. (1992). The nonlinear Schrödinger limit and the initial layer of the Zakharov equations. *Diff. Int. Eqn.* **5,** 721–745.
20. Payne, G. L., Nicholson, D. R., and Downie, R. M. (1983). Numerical solution of the Zakharov system. *J. Comput. Phys.* **50,** 482–498.
21. Schochet, S., and Weinstein, M. (1986). The nonlinear Schrödinger limit of the Zakharov equations governing Langmuir turbulence. *Comm. Math. Phys.* **106,** 569–580.
22. Strang, G. (1968). On the construction and comparison of difference schemes. *SIAM J. Numer. Anal.* **5**(3), 506–517.
23. Sulem, C., and Sulem, P. L. (1999). The nonlinear Schrödinger equation. Springer-Verlag, New York.